[14] The synthesis of siloxantphos (**A**) and siloxPNP (**C**) will be published elsewhere.
[15] ^{31}P NMR (121.4 MHz, D_2O, H_3PO_4): [Rh(xantphos)(acac)CO]: $\delta = 13$ (d, $J_{P-Rh} = 94$ Hz); [Rh(xantphos)CO]$^+$: $\delta = 37$ (d, $J_{P-Rh} = 121$ Hz).
[16] The stretch frequency of the carbonyl group is slightly influenced by the nature of the counterion of the complexes.
[17] J. W. Niemantsverdriet, *Spectroscopy in Catalysis*, VCH, Weinheim, **1995**.
[18] M. Besson, P. Gallezot, C. Pinel, S. Neto, *Heterog. Catal. Fine Chem. Proc. Int. Symp. IV* **1997**, 215–222.
[19] Crystal structure determination of **2**(BF_4): $C_{40}H_{32}O_2P_2Rh \cdot BF_4 \cdot 0.5\,CH_2Cl_2$, $M_r = 838.78$, yellow needle, $0.75 \times 0.25 \times 0.08$ mm^3, triclinic, space group $P\bar{1}$ (no. 2), $a = 11.5217(10)$, $b = 12.4937(13)$, $c = 13.003(2)$ Å, $\alpha = 91.954(11)$, $\beta = 89.957(11)$, $\gamma = 106.025(8)^\circ$, $V = 1797.9(4)$ Å^3, $Z = 2$, $\rho = 1.549$ g cm^{-3}, $\mu = 0.695$ mm^{-1}. A total of 8558 reflections were measured on an Enraf-Nonius CAD4T diffractometer with rotating anode ($\lambda = 0.71073$ Å) at a temperature of 150(2) K; 8148 reflections were unique ($R_{int} = 0.0483$). The structure was solved with direct methods (SIR97) and refined with SHELXL97 against F^2. R values [$I > 2\sigma(I)$]: $R1 = 0.0538$, $wR2 = 0.1337$. Crystallographic data (excluding structure factors) for the structures reported in this paper have been deposited with the Cambridge Crystallographic Data Centre as supplementary publication no. CCDC-128890. Copies of the data can be obtained free of charge on application to CCDC, 12 Union Road, Cambridge CB2 1EZ, UK (fax: (+44) 1223-336-033; e-mail: deposit@ccdc.cam.ac.uk).
[20] N. W. Alcock, J. M. Brown, J. C. Jeffery, *J. Chem. Soc. Dalton Trans.* **1976**, 583–588.
[21] The bite angles of the ligands were calculated on [Rh(ligand)] as reported in ref. [12].
[22] See the Supporting Information for the determination of the rate equation.

Visualization of Surface Gelation Processes in a Doped Sol–Gel Glass

Germain Puccetti* and Roger M. Leblanc

Sol–gel materials present an alternative to organic polymers and have the advantage of operating at room temperature. This makes them particularly interesting for doping with biological materials.[1, 2] Much work on the chemistry of sol–gel materials aims at adjusting the initial sol composition to control the hydrolysis and condensation reactions according to the desired application of the end material. In situ studies of the evolution of a sol–gel in thin films are based on the optical (for example, fluorescence, interferometry) or mechanical properties (for example, stress) and yield macroscopic information from which the material evolution is inferred.[3–5] Thin-film fabrication is particularly sensitive to the initial chemistry because of the strong influence of environmental constrains over the large exposed surface (air humidity, solvent evaporation).[6–8]

[*] Dr. G. Puccetti, Prof. Dr. R. M. Leblanc
Center for Supramolecular Science and Department of Chemistry
University of Miami
P.O. Box 249118 Coral Gables, FL 33124–0431 (USA)
Fax: (+1) 305-284-1880
E-mail: gpuccett@umiami.ir.miami.edu

The present work reports the first depth-resolved, in situ measurements of the near-surface regions of a material during its evolution from the sol to the gel states. The organic dye molecule β-carotene serves as a probe for the chemical changes that occur during the sol–gel evolution. Depth analysis evidences a clearly distinct chemical evolution at the surface of the material relative to the bulk. This is attributed to the exposition of the surface to air.

Photoacoustic spectroscopy (PAS) relies on optical excitation of a material and measurement of the induced heat release. Despite its simple basic principles, PAS covers a broad range of phenomena that occur during the process of converting absorbed light into the release of heat. Several information factors can be identified that influence, directly or indirectly, the energy conversion process: a) the light absorption coefficient; b) the molecular-level de-excitation process; c) the excitation/heat transfer to the molecular environment; d) heat propagation; and e) the spatial distribution of microscopic heat sources inside the sample. The characterization of any material by PAS is governed by three main material properties: 1) the light absorption distribution (Beer's law); 2) the thermal diffusion; and 3) the thickness of the material being investigated.[9, 10]

The relative importance of the aforementioned information factors can be modified by choosing sample conditions so as to eliminate some of them.[11] In the present study, thin samples and a low dopant concentration allow us to neglect three out of the five factors. Two dominant information factors influence the response signal: energy transfer from β-carotene to its microscopic environment (c) and variable thermal properties of the sample (d). However, a previous study has shown that the changes in the thermal property of the sample (during the sol to gel evolution) are small with respect to the energy transfer factor.[11] The measured signal is therefore dominated by changes in the efficiency of heat transfer from β-carotene molecules to their immediate molecular environment. This dopant molecule was chosen because of its very good stability in sol–gel materials and its near unit thermal de-excitation conversion yield.[12–14]

A thicker sample (about 1 mm) was used initially to simulate bulk sol–gel material during its chemical aging. The depth-dependent heat emission that was extracted from the time response signal, obtained from pulsed photoacoustic spectroscopy (PPAS), versus time of aging is given in Figure 1b. The classical PPAS signal (Δp_{max}, t_{max}) is added for comparison (Figure 1a). Studies of the dopant dynamics of a tetramethoxysilane (TMOS)/dimethylaminopyridine (DMAP) sol–gel have shown that the sol phase is characterized by an increase in length of polymers with time which results in an increasing viscosity of the medium.[15] Macroscopic gelation occurs when the longer polymer species are consumed to form the long-distance network. This process results in a temporary decrease in hindrance (local viscosity) around dopant molecules and β-carotene experiences a sudden return to a solventlike environment.

The depth-resolved signal (Figure 1b) reveals two distinct time evolutions: near the sample surface (less than 11 μm) and in its bulk (greater than 11 μm). These were not apparent on the global response signal (Figure 1a) as obtained by classical

  1433-7851/99/3821-3235 $ 17.50+.50/0

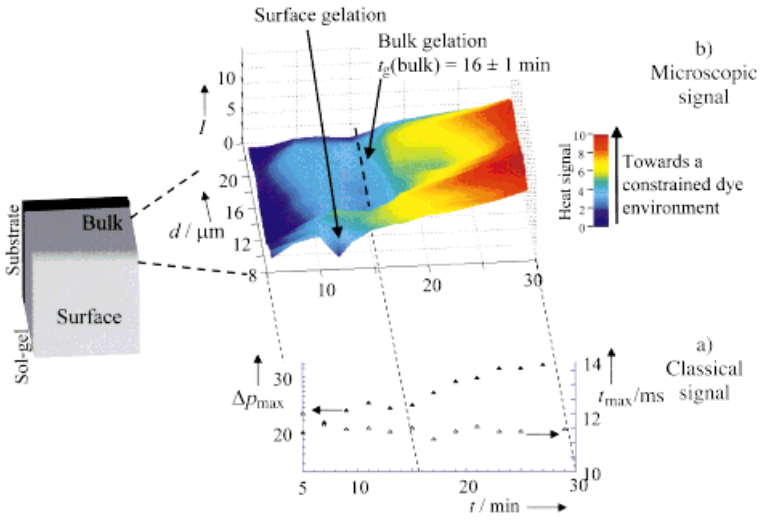

Figure 1. Surface and bulk sol–gel processes in a thick sample: A massive material. a) The classical PPAS response signal (Δp_{max} and t_{max}) is presented versus time; b) the depth-analyzed signal extracted from the PPAS responses of (a) is given versus time t and depth d (also μ_D) in the upper part of the figure. In the sample view on the left the bulk material is represented by dark gray and the environment-influenced surface layer of the material by light gray.

PPAS. A faster evolution is observed near the sample surface (gelation time $t_g = 12$ min) than in its bulk ($t_g = 16$ min). This result is a consequence of solvent (alcohol) evaporation at the surface, which depletes the amount of methanol and results in a higher precursor concentration (equivalent to a higher initial molar ratio). A faster surface evaporation is therefore consistent with a higher reactivity as a result of a local increase in the concentration of the precursor. The gelation remains quite constant with depth in the bulk region (depths greater than 12 µm) of the sol–gel. This observation is consistent with a pure interfacial effect and shows that the solvent evaporation affects only a surface layer of about 10–12 µm thickness. The absence of any gelation transition for a depth around 11 µm could be the result of a solvent concentration gradient as the inside of the gel plays the role of reservoir in supplying the surface regions, driven by high evaporation rates. The depression occurring near a depth of 14–18 µm and at times of 18–24 min could be attributed to solvent accumulation resulting from the dense silicon surface.

In a second experiment, a thin sample (about 80 µm, Figure 2) was chosen to reduce the contribution of the bulk gelation and enhance the signal contribution from the surface. The low viscosity of the initial sol meant that a simple drop deposition of the sol on the sapphire substrate could be used for the preparation of a homogeneous layer. Because of its reduced bulk content, this second sample is also expected to limit solvent effects. For a better time resolution, the evolution was slowed down by halving the DMAP concentration. Contrary to the previous massive sample, the film sample shows one clear transition near the surface. The depth analysis with time (Figure 2b) shows a well contrasted surface evolution ($t_g = 13$ min). A residual bulk gelation can be slightly observed around 42 min (also obtained from observation of a laboratory experiment carried out in a vial), which confirms our hypothesis of a film sample, that is, independent of a bulk component. The similar values of both surface gelation processes indicates that its chemistry is dominated by a precursor densification effect. The absence of transition in deeper layers indicates few chemical changes occurring after the first instants. The very fast depletion of solvent molecules induces a solidlike environment for dopant molecules. The classical response signal amplitude Δp_{max} (Figure 2a) shows a similar increase with time of aging as observed for the massive sample. This is due to a progressive solid network formation that leads to an improved propagation of heat from the inside to the surface.[8]

The present results show that information hidden by the total signal evolution can be extracted from a simplified model and converted into a depth profile of the microscopic heat emission. This analysis has revealed a completely different surface evolution that is driven mainly by a densification of the precursor molecules. This is, to our knowledge, the first in situ observation of clearly separate surface and bulk gelation processes in a sol–gel material.

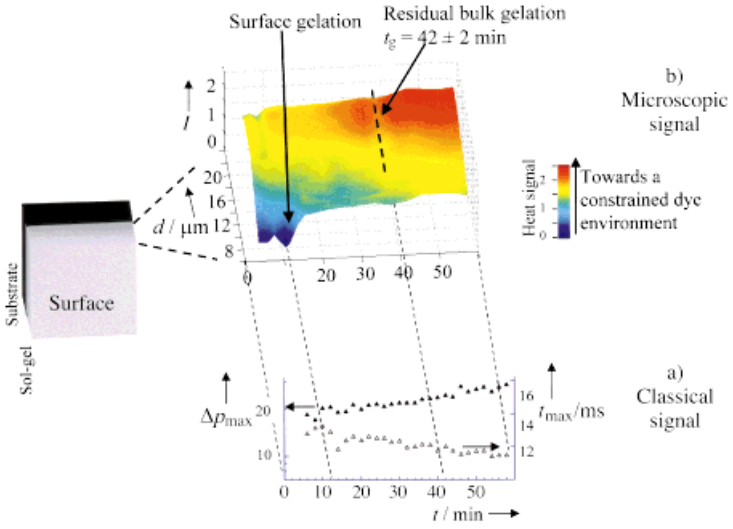

Figure 2. Surface dominated sol–gel materials: The case of a thin sample. a) The classical PPAS response signal (Δp_{max} and t_{max}) is presented versus time; b) the depth-analyzed signal extracted from the PPAS responses of (a) is given versus time t and depth d (also μ_D), in the upper part of the figure. The sample is represented by a dominant light gray shade to show that the material evolution is influenced by surface effects.

An in situ monitoring could be particularly important for applications of thin films of sol–gel materials such as in integrated optics or for enzymes entrapped in biosensor films.

Experimental section

The sol–gel materials were composed of tetramethoxysilane/water/ethanol/dimethylaminopyridine with respective molar ratios 1:7:4:x, where x was doped with β-carotene at the concentration of 10^{-4} M in the solution state. By adjusting x to 0.002 or 0.001 gels within t_g(bulk) = 16 or 42 min were obtained. The procedure was reported elsewhere.[16] We chose the drop-deposition technique for the thick-film sample because it can be prepared in the measurement cell and allows for measurements at very short times. The deposition reliability, hence the measurement reproduci-

  1433-7851/99/3821-3236 $ 17.50+.50/0

bility, were insured by performing deposition of a 60 μL drop (by a calibrated micropipet) onto an inclined PAS cell. A small reservoir around the slightly protruding sapphire window collects the excess sol liquid and helps ensure a reproducible film thickness. This method of deposition was compared to dip coating of the sol onto a thin quartz plate and was found to give information at earlier times as a result of the limited handling time involved. Temperature and humidity conditions were kept similar between experiments (19 °C and 60 % relative humidity, respectively).

Pulsed photoacoustic spectroscopy (PPAS) was used for time resolution by exciting samples with 532 nm radiation. We chose a sample thickness (1 mm) and a dopant concentration (10^{-4} M) to characterize our material as a thermally thick and optically transparent case. Fourier spectra obtained from the PPAS response pulses showed a $1/f$ dependence (f = Fourier frequency). The PAS response signal in Fourier space is also proportional to the yield for the conversion of the energy of absorbed light into released heat η integrated over the thickness $z(f)=\mu_D(f)$ of material being detected.[10, 17, 18]

It is then possible to infer the local signal contribution at a given depth $z_i+\delta z/2$ by differentiation of the PAS signals corresponding to the two neighbor layers of thicknesses $z_i=\mu_D(f_i)$ and $z_i+\delta z=\mu_D(f_{i+\delta i})$ ($0<\delta z\ll z_i$, $f_i>f_{i+\delta i}$) [Eq. (1)] by using a mixture law for $\eta(f_{i+\delta i})$ and $\eta(f_i)$ (Figure 3).

$$\eta(\delta z)=\frac{1}{\Delta\mu_D}\mu_D(f_{i+\delta i})(\eta(\Delta p(f_{i+\delta i}),f_{i+\delta i},\rho_{i+\delta i},k_{i+\delta i},C_{i+\delta i}) - \frac{\mu_D(f_i)}{\mu_D(f_{i+\delta i})}\eta(\Delta p(f_i),f_i,\rho_i,k_i,C_i)) \quad (1)$$

Several steps are involved in the determination of the depth profile: conversion of the time signal into a frequency-dependent signal ($\Delta p(f)$) by Fourier transformation, extraction of the local heat signal η by differentiation between neighboring layers (Figure 3), and relating the Fourier frequency f to the depth μ_D by using the thermal properties of the material ($\mu_D(f)=(k/\rho Cf)^{0.5}$).

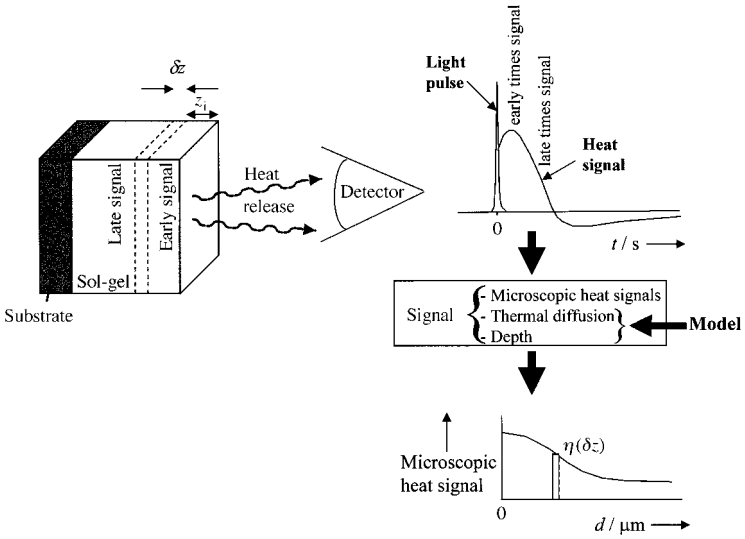

Figure 3. Schematic representation of the dependence of the signal on the depth of heat release inside the sol–gel. The global signal is converted, by fast Fourier transform (FFT) and a model, into a microscopic heat signal versus depth d. The local depth-resolved signal from a layer at a depth $z_i+\delta z/2$ results from the differentiation of signals from the two surrounding layers of thicknesses z_i and $z_i+\delta z$.

The signal analysis was performed using a sample with a mixed methanol/alkoxide composition (density $\rho=0.9\,g\,mL^{-1}$, heat capacity $k=2.5\,mW\,cm^{-1}\,K^{-1}$, and thermal conductivity $C=2.0\,J\,g^{-1}\,K^{-1}$). The resulting local heat release (microscopic signal) is presented versus the depth, as calculated from thermal diffusion lengths. Modifications of thermal parameters, for example, resulting from a surface gradient, were found to have a negligible effect on the observed effects. For comparison the global PPAS response signals ($\Delta p_{max}(t)$ and the time delay of the pulse maxima t_{max}) were added to these figures as a function of time.[11]

The influence of depth-dependent thermal properties on the signal was also investigated by using an exponential variation (between a dominant alkoxide composition and the previous mixed one) over a thickness of 12 μm (inferred from the previous analysis). Results showed little changes with respect to the first representation and are therefore not included here. Finally, any increase in light absorption near the surface of the sample as a result of increased dopant concentration was found to be negligible, as evident from the previous observation that no major variations in signal amplitude versus depths occur (Figure 1).

Received: March 19, 1999 [Z13191IE]
German version: *Angew. Chem.* **1999**, *111*, 3425–3428

Keywords: dyes · glasses · photoacoustic spectroscopy · sol–gel processes

[1] J. D. Jordan, R. A. Dunbar, F. V. Bright, *Anal. Chem.* **1996**, *67*, 2436.
[2] D. Avnir, S. Braun, O. Lev, M. Ottolenghi, *Chem. Mater.* **1994**, *6*, 1605.
[3] J. I. Zink, B. S. Dunn, B. C. Dave, F. Akbarian, *Mater. Res. Soc. Symp. Proc.* **1996**, *435*, 187.
[4] B. C. Dave, B. S. Dunn, F. Leroux, L. F. Nazar, H. P. Wong, *Mater. Res. Soc. Symp. Proc.* **1996**, *435*, 611.
[5] F. Nishida, *J. Am. Ceram. Soc.* **1995**, *78*, 1640.
[6] L. C. Klein, *Sol–gel Technology for Thin Films, Fibers, Preforms, Electronics, and Specialty Shapes*, Noyes, Park Ridge, **1988**.
[7] C. J. Brinker, G. W. Scherer, *Sol–gel Science*, Academic Press, New York, **1989**.
[8] L. L. Hench, J. K. West, *Chem. Rev.* **1990**, *90*, 33.
[9] A. Rosencwaig, A. Gersho, *J. Appl. Phys.* **1976**, *47*, 64.
[10] A. Mandelis, B. S. H. Royce, *J. Appl. Phys.* **1979**, *50*, 4330.
[11] The thermal transmittance of a sol–gel sample was measured with time by excitation of a black carbon backing in contact with the sample by PPAS. Results have shown signal variations smaller than 5 % of the total signal, and therefore demonstrates the weak influence of thermal properties on the actual measured signal. G. Puccetti, R. M. Leblanc, *J. Non Cryst. Solids*, in press.
[12] D. Avnir, *Acc. Chem. Res.* **1995**, *28*, 328.
[13] F. Nishida, J. M. McKiernan, B. Dunn, J. I. Zink, C. J. Brinker, A. J. Hurd, *J. Am. Ceram. Soc.* **1995**, *78*, 1640.
[14] L. R. Reisfeld, C. K. Jorgensen, *Chemistry, Spectroscopy and Applications of Sol–gel Glasses*, Springer, Berlin, **1995**.
[15] P. Griesmar, C. Sanchez, G. Puccetti, I. Ledoux, J. Zyss, *Mol. Eng.* **1991**, *1*, 205.
[16] G. Puccetti, R. M. Leblanc, *J. Phys. Chem.* **1996**, *100*, 1731.
[17] D. L. Balageas, J. C. Krapez, P. Cielo, *J. Appl. Phys.* **1986**, *59*, 348.
[18] G. Puccetti, R. M. Leblanc, *J. Phys. Chem.* **1998**, *102*, 9002.

  1433-7851/99/3821-3237 $ 17.50+.50/0